ARTICLE NO. 78-1075R

A80-037

Results of Experimental Investigations of the L^* Phenomenon

60003
60012

H.F.R. Schöyer
Delft University of Technology, Delft, The Netherlands

L^* instability manifests itself as chuffing, low-frequency bulk mode oscillations, and dp/dt extinguishment. Experiments were conducted with two types of double-base propellant and with a composite propellant, using two L^* burners, one with a 5 cm i.d. and the other with 10 cm i.d. The results obtained with both burners correlate well. It was observed that ignition has a strong influence on the occurrence and type of L^* instability; hence, a reproducible ignition technique was developed. An accurate reduction of the large amount of data is done by means of a computer program which was developed especially for this purpose. Chuffing was observed, with all propellants; oscillatory combustion, though different in appearance, occurred with one double-base and with the composite propellant, while dp/dt extinguishment was observed only with the composite propellant. There is experimental evidence that the imaginary part of the propellant response function depends upon the frequency of the oscillations, while the mean pressure and frequency of L^* oscillations are related. Stability boundaries were estimated from the data.

Nomenclature

A	= area
a	= coefficient in burning rate law
C	= proportionality constant
D	= diameter of L^* burner
d	= diameter
F	= frequency
L^*	= characteristic length
MBE	= mean boundary for dp/dt extinguishment
MSB	= mean stability boundary
n	= exponent in burning rate law
P	= period
p	= pressure
R	= gas constant of combustion products
R_b^i	= imaginary part of propellant response function
r	= burning rate
T	= term in Eq. (9) = A or V
T_c	= adiabatic flame temperature
t	= time
V	= chamber volume
α	= growth constant
γ	= ratio of specific heats
Γ	= Vandenkerckhove function of γ

Subscripts

d	= dampening
eff	= effective
f	= final
i	= ith local pressure maximum
im	= ith local pressure minimum
in	= initial
t	= nozzle throat
$\bar{()}$	= mean value
Δ	= increment

Received June 29, 1978; presented as Paper 78-1075 at the AIAA/SAE 14th Joint Propulsion Conference, Las Vegas, Nev., July 25-27, 1978; revision received Oct. 9, 1979. Copyright © American Institute of Aeronautics and Astronautics, Inc., 1978. All rights reserved. Reprints of this article may be ordered from AIAA Special Publications, 1290 Avenue of the Americas, New York, N.Y. 10019. Order by Article No. at top of page. Member price $2.00 each, nonmember, $3.00 each. **Remittance must accompany order.**

Index categories: Combustion Stability, Ignition, and Detonation; Solid and Hybrid Rocket Engines.

*Senior Faculty Member, Dept. of Aerospace Engineering; Consultant, National Defense Organization, T.N.O. Member AIAA.

Introduction

L^* INSTABILITY has been a well-known phenomenon in solid rocket technology for many years, and may be divided into chuffing, oscillatory combustion, and dp/dt extinguishment. Chuffing is the succession of very short periods of burning, during which the pressure rises well above the ambient level, but no steady-state burning is reached. Extinction rapidly follows ignition and the sequence is repeated, often many times. Oscillatory combustion during L^* instability is of the bulk mode type where the oscillation is in phase at every location in the combustion chamber. Various amplitude histories may be observed. Typical patterns are:

1) After a rapid rise in pressure to a mean level, large amplitude oscillations occur. The amplitude decreases continuously until steady burning takes place.

2) After a more or less regular pressure buildup, growing oscillations occur which level off. After a short time these oscillations decay until steady combustion takes place.

3) After a more or less regular rise in pressure, growing amplitudes are observed followed by extinguishment. Often after a short interval reignition occurs. The extinguishment which follows the large amplitude oscillations is known as dp/dt extinguishment.

Akiba and Tanno[1] and Sehgal and Strand[2] analyzed low-frequency combustion instability in their classic papers. The residence time of the combustion products in the chamber depends on the chamber geometry, or L^*, and on thero-modynamic properties of the combustion products, but not on the pressure. Between a pressure fluctuation and the resulting burning rate fluctuation, there is a time lag, and the low-frequency oscillation results as a coupling between this time lag and the residence time. Oberg[3] and Culick[4] showed that these oscillations may be regarded as a kind of acoustic oscillations and are of the bulkmode type.

Ignition has a strong influence on the occurrence of L^* instability. To obtain reliable and reproducible results ignition technique is very important.

To investigate L^* instability, experiments may be carried out in small, end-burning motors. These test motors, L^* burners, have an adjustable chamber geometry and employ interchangeable nozzles so that the primary test variables—characteristic length L^*, and mean pressure $\bar{p}$—may be adjusted to required values. For the present series of experiments, two L^* burners of different size were used. This allows investigation whether scale effects have an influence on the occurrence of L^* instability. Double base and composite

propellants were used and though very different in nature, these propellants display many similar characteristics insofar as L^* instability is concerned.

Experimental Facilities

The L^* burner consists of a cylindrical combustion chamber closed at one end by a nozzle end plate holding a nozzle. A number of different nozzles are available and the choice of a specific nozzle, in combination with the propellant, determines the steady-state operation pressure. At the other end, the combustion chamber is closed by a piston to which a circular disk of propellant is bonded. The propellant is ignited at its exposed surface. Ideally, the L^* burner is a cigarrette burning motor, with a constant burning surface.

The distance from the piston to the nozzle end plate is adjustable. The characteristic length L^* follows from the ratio of chamber volume to nozzle throat area:

$$L^* = V/A_t \tag{1}$$

As propellant is consumed, the characteristic length L^* increases.

The chamber pressure can be measured at two different locations: at the nozzle end plate and at the piston directly behind the propellant. For the latter location, care must be taken to assure a good contact between the rear surface of the propellant and the transducer.

Two L^* burners were manufactured, one with an internal diameter of 5 cm, and one with an i.d. of 10 cm. They are denoted as the 5 cm and 10 cm L^* burners, respectively.

A cross section of the 5 cm L^* burner is shown in Fig. 1, and described in detail by De Boer and Schöyer.[5] There is a close resemblance to the 2.5 in. i.d. L^* burner in use at the Jet Propulsion Laboratory.

Pressure is measured, either by one or two piezoelectric Kistler pressure transducers or by strain gage transducers. Signals are recorded by an oscillograph and on magnetic tape by an FM instrumentation tape recorder. The signal on magnetic tape allows replay at different speeds and amplifier settings to enlarge interesting features of the pressure oscillations and digitizing of the recorded signal for computerized data reduction.

All L^* experiments were conducted with propellant disks cut from available propellant grains, bonded to the piston, and machined to size. Inhibitor was applied to the periphery of the disk and finally a NiChrome ignition wire was placed on the flat face of the disk and covered with igniter paste.

Ignition Method

For reliable results, the experiments should be reproducible. Many experimenters mention poor reproducibility.[7] It was recognized at an early stage of our research program that ignition has a strong influence on the reproducibility of the experiments, on the occurrence of L^* oscillations, and on chuffing. For example, a high pressure peak may trigger oscillations which, in the absence of such a peak or with a much lower pressure peak, would not have appeared, while too low an ignition pressure may result in chuffing. Various ignition procedures were tried[5] including combinations of ground propellant and blackpowder, squibs, ignition wires bonded to the propellant, or ground propellant contained in cartridges; in none of these cases could satisfactory results be obtained. Either high ignition peaks occurred, the results were irreproducible, or ignition was too slow. Finally a lacquer paste painted on the propellant surface over a NiChrome resistance wire produced smooth ignition and reproducible pressure histories during test runs.

In the majority of cases instantaneous ignition over the whole propellant surface was achieved so that the burned surface remained flat. The paste is easy to apply and is compatible with the propellants. The composition of the successful pyrotechnic lacquer is given in Table 1. After its development this ignition method was used with all test runs and is well suited for experimental purposes because the ignition peak is low (usually below 0.5 MPa).

Data Reduction

All experiments with double base propellants were reduced "manually," using a scale to read time and pressure to accuracy of about 0.25 mm. Before each series of test runs, the pressure transducers and amplifiers were calibrated to ensure accurate measurements.

Figure 2 is a schematic of a pressure history. Usually, neither the amplitude nor the frequency of the oscillations is constant during L^* oscillations. Therefore, to avoid confusion and misinterpretations, the amplitude and frequency during oscillations must be defined clearly, without ambiguity.

The time to which a variable is related during pressure oscillations is the instant at which a pressure peak occurs. The oscillation period is defined as the time between two successive pressure peaks, i.e.,

$$P(t_i) = P_i = t_{i+1} - t_i \tag{2}$$

The pressure amplitude and mean pressure at an instant t_i are defined accordingly (see Fig. 2):

$$\Delta p_i = (p_i - p_{im})/2 \tag{3}$$

$$\overline{p_i} = (p_i + p_{im})/2 \tag{4}$$

Other definitions are possible, but no specific advantages are seen. The pressure dependence of the propellant burning rate is expressed as

$$r = ap^n \tag{5}$$

for the appropriate pressure intervals. It is known that such relationships hold only for steady pressures, but for lack of other relationships Eq. (5) is used to estimate the instantaneous characteristic length L^*.

As the initial distance of the propellant surface to the nozzle end plate L_{in} is known, L_i^* follows from

$$L_i^{*(I)} = \left(\frac{D}{d_t}\right)^2 \left(L_{in} + \int_0^{t_i} r\,dt\right) \tag{6}$$

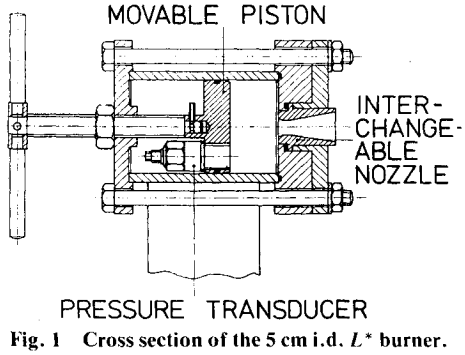

Fig. 1 Cross section of the 5 cm i.d. L^* burner.

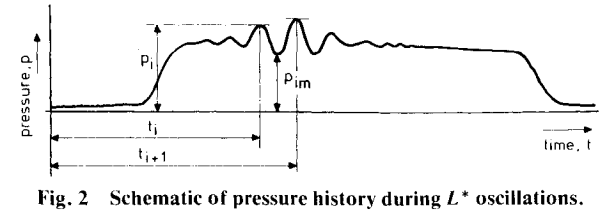

Fig. 2 Schematic of pressure history during L^* oscillations.

If, after ignition, chuffing occurs, it is difficult to estimate how much propellant was consumed before oscillations start. One may also have several series of oscillatory combustion in one test run and in such cases an estimate of the amount of propellant consumed may become inaccurate. After final extinguishment, the distance L_f of the propellant to the nozzle end plate is measured to obtain the final characteristic length L_f^*. This yields an alternative way to determine L_i^*:

$$L_i^{*(2)} = \left(\frac{D}{d_t}\right)^2 \left(L_f + \int_{t_f}^{t_i} r\,dt\right) \tag{7}$$

Usually, $L_i^{*(1)}$ and $L_i^{*(2)}$ differ due to 1) the use of the steady-state burning rate law, which does not hold during oscillatory combustion, 2) inaccuracies in the integration, and 3) measurement inaccuracies.

However, with manual data reduction improvement is hardly possible. Therefore, a faster and more accurate means of data reduction is employed using a digital computer. The analog signal is digitized and a special computer program utilized[8] which, among other features, has the capacity to distinquish the tops and bottoms of the oscillations, and therefore can determine, in a manner analogous to the manual data reduction, mean pressure, pressure amplitude, frequency, the amount of propellant consumed, and the instaneous L^*. A purely digital determination of the frequency and amplitude of the oscillations obtained by recognizing tops and bottoms proved more efficient than a Fourier analysis, as neither the amplitude nor the frequency during a test run remains constant. This method of computerized data reduction was applied to the experiments with composite propellants. The difference between L_{in}^* as calculated and L_{in}^* that follows from the experimental data (and similarly for L_f^*) is minimized by "stretching" or compressing the L^* data so that the calculated and measured L^* values at both ends of the interval coincide.

Double-Base Propellants

Often L^* instabilities are classified as chuffing, oscillatory combustion, and dp/dt extinguishment[9]; however, no dp/dt extinguishment was observed during experiments with double-base propellants. Two types of double-base propellants were used, JPN and ARP, and their compositions are listed in Table 2.

Table 1 Composition (wt. %) of successful pyrotechnic lacquer and PH 5179 propellant

Ingredients of pyrotechnic lacquer:		Ingredients of PH 5179 propellant:	
Potassium-nitrate	20	Cellulose-nitrate	52.7
Blackpowder (meal)	10	Glycerol-tri-nitrate	42.85
Silicon	20	Centralite I (ethyl)	2
Solution of 75 g	50	Vaseline	0.45
PH 5179 propellant		Potassium nitrate	1.5
in 1000 cm^3 acetone		Graphite	0.15
		Moist	0.35

Table 2 Composition (wt. %) of JPN and ARP propellants

	JPN	ARP
Cellulose-nitrate	51.22	49.9
Glycerol-tri-nitrate	43	36.4
Tri-acetin		4
Di-ethylphtalate	3.25	
Ethylcentralite	1	
Lead salts		4
Additives	1.53	5.7

JPN Propellant

Oscillatory combustion was observed in only 4 of 65 test runs. It was found that high ignition peaks may trigger L^* oscillations. The experiments with JPN propellant were mainly conducted with pyrotechnic mixtures for ignition. That the ignition spike can trigger L^* oscillations is clearly illustrated by Fig. 3 which shows two test runs, 303A and 303B. Conditions for the test runs were identical. Igniters were cartridges with 1 and 2 g of ignition mixtures and the resulting ignition pressures were 0.3 and 2.2 MPa which makes the difference between a smooth combustion and the occurrence of L^* oscillations. Later experiments which used the pyrotechnic lacquer did not show oscillations.

In only one case was sustained oscillatory combustion observed (Fig. 4) where it is seen that a high ignition pressure peak is present (6.1 MPa). It is believed that the high ignition peak triggered the oscillations. If the pressure amplitude grows as $p' = p_0' e^{\alpha t}$, α is called the growth constant. For this particular experiment, the growth constant is $\alpha = 1.9\ s^{-1}$.

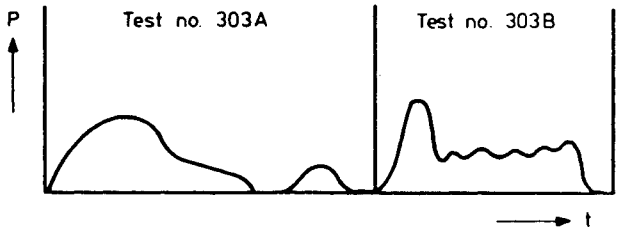

Fig. 3 Ignition spikes may trigger L^* instability.

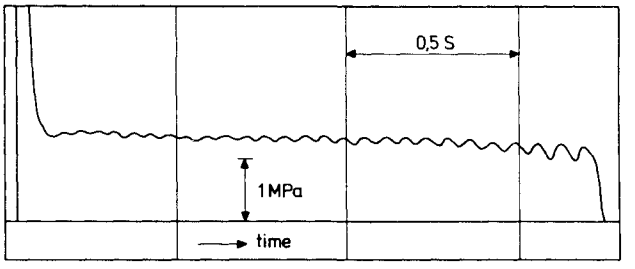

Fig. 4 L^*oscillations of JPN propellant.

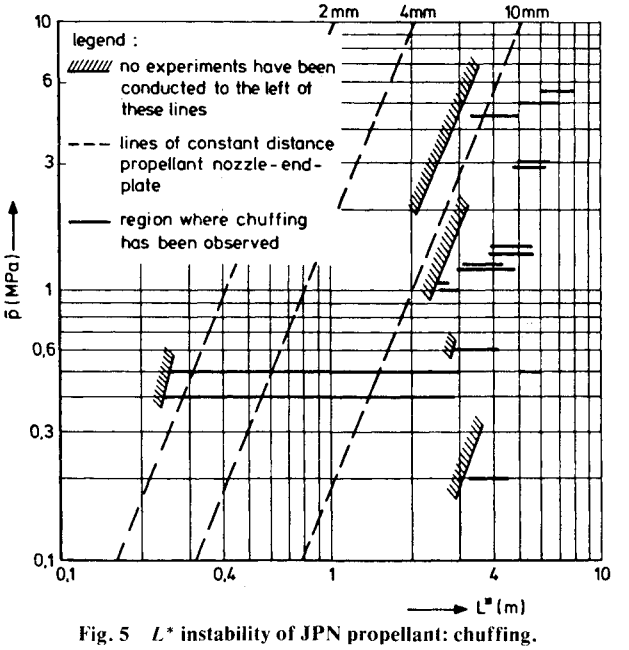

Fig. 5 L^* instability of JPN propellant: chuffing.

Chuffing was observed during many experiments with numerous repetitions and in some cases more than 30 successive chuffs were counted before combustion ceased. The solid horizontal lines in Fig. 5 indicate, approximately, the regimes where chuffing of JPN propellant was observed. The oblique lines refer to constant distances from the propellant to the nozzle end plate. No tests were conducted to the left of the hatched boundaries. This figure implies that there is a connected region in the $L^* - \bar{p}$ plane where chuffing of JPN propellant may be expected. The figure is only qualitative as it is difficult to estimate accurately the mean pressure during chuffs, and also the L^* range can only be estimated roughly.

ARP Propellant

L^* oscillations were observed during 7 of 60 test runs with ARP propellant.[5,10] All test runs showing oscillations were ignited by the pyrotechnic lacquer and the ignition peaks were low (between 0.2 and 0.4 MPa). In all cases ignition was followed by chuffs (between 4 and 81) before the definite pressure buildup occurred.

In general, oscillations started before equilibrium (mean) pressure was reached. It may be that the oscillatory nature of combustion delayed the moment at which equilibrium (mean) pressure was reached, but it is also conceivable that the propellant surface was not yet fully ignited and this phenomenon might be attributed to flame spreading. A typical pressure history observed during oscillatory combustion of ARP propellant in the 10 cm L^* burner is presented in Fig. 6.

Figure 7 shows L^* oscillations obtained during a test run conducted at about the same pressure and L^* ranges as the test run of Fig. 6 but in the 5 cm L^* burner. Although not exact replicas of each other, the figures are very much alike and display many similar features, which were also observed in other test runs[10]:

1) After the initial pressure rise, the pressure levels off for a short period at about 0.5 MPa. At this low pressure level high frequency, small amplitude oscillations are seen.

2) The low pressure level is followed by a rise in mean pressure upon which pressure oscillations with a rather large amplitude are visible.

3) After equilibrium pressure is reached, the oscillations rapidly decay and steady burning results.

The observed normalized pressure amplitude and frequency of the test run of Fig. 6 are shown in the Figs. 8 and 9. It may be seen from these figures that at the very beginning the pressure amplitude is small and the frequency is high. Moreover, the low frequency part of the pressure amplitude history (Fig. 8) is seen to be more or less parabolic on the logarithmic scale, while the frequency itself (Fig. 9) appears to

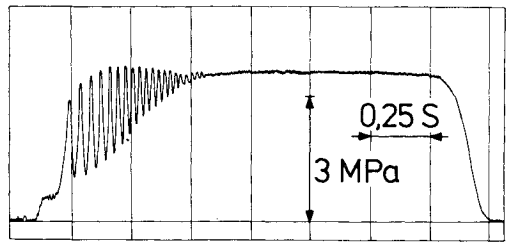

Fig. 6 L^* oscillations of ARP propellant (10 cm L^* burner).

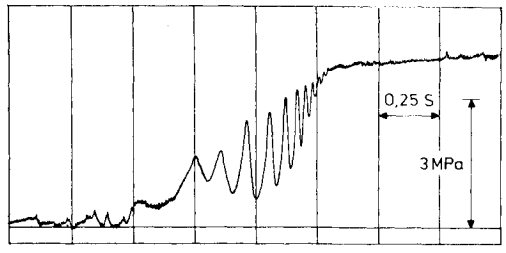

Fig. 7 L^* oscillations of ARP propellant (5 cm L^* burner).

increase almost linearly with time. This last phenomenon was observed during most cases of oscillatory combustion of ARP propellant.

An effective growth constant may be estimated from Fig. 8 for ARP, although this may not be too meaningful because $\ln(\Delta p/\bar{p})$ is not very linear with time. In this respect, one should recall that the definition of the growth constant assumes a constant mean pressure. In the present experiments the time scale of mean pressure is about an order of magnitude larger than the period of the oscillations[10] (cf. Figs. 6 and 7), therefore the mean pressure may be assumed constant for the determination of the growth constant based on $\Delta p/\bar{p}$. All experiments were analyzed in this way and the results are given in Table 3.

Nearly all effective growth constants are negative, i.e., the oscillations start at about full amplitude and then decay.

An attempt was made to estimate the propellant growth constants by comparing the results of different experiments. Using two L^* burners of different size, it was possible to repeat experiments at about the same L^* and combustion pressure with different chamber volumes. If the losses depend upon geometrical quantities the dampening constant may be estimated.

It is assumed that the effective growth constant α_{eff} is the difference between the propellant growth constant and the

Table 3 Effective growth constant and frequency during oscillatory combustion of ARP propellant in 5 and 10 cm L^* burners

Test no.	Diam. of L^* burner, cm	Effective growth constant α_{eff}, s^{-1}	Frequency range F, s^{-1}	Mean pressure range, MPa	L^* range, m
936[I]	5	...	50-75	0.31-0.39	0.8-0.84
936[II]	5	...	45-55	0.13-0.23	0.85-0.86
936[III]	5	-2.79	18-28	1.95-2.36	1.1-1.5
950	10	-1.21	12-33	1.92-2.36	0.43-0.78
950	10	-9.20	12-33	2.36-2.85	0.78-1.13
951	10	...	87-93	0.40-0.49	0.29
951	10	...	77-84	0.66-0.72	0.32-0.33
951	10	-7.53	26-45	2.18-3.81	0.39-1.24
952	10	-16.92	30-35	2.79-2.96	1.48-1.66
953	10	-12.90	20-40	2.50-3.35	0.31-0.60
953	10	...	40-45	3.53-3.71	0.71-0.79
953	10	...	45-51	3.84-3.85	0.90-0.97
955	5	5.70	60-75	0.52-0.55	0.36-0.40
955	5	-4.07	9-11	1.38-1.63	0.49-0.73
955	5	-43.56	15-51	1.93-3.76	0.84-1.23
956	5	-28.79	25-36	2.41-2.90	0.80-0.95

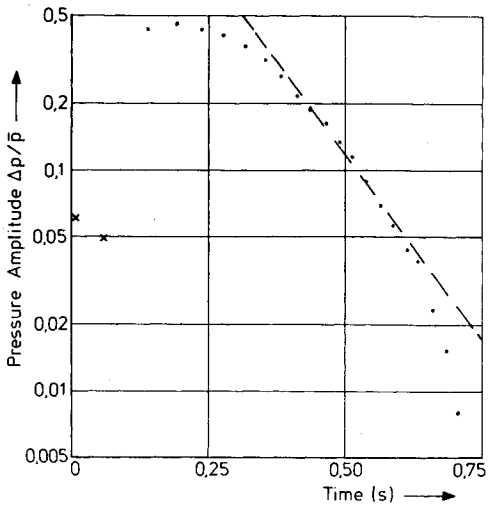

Fig. 8 Normalized pressure amplitude during L^* oscillations of ARP propellant (10 cm L^* burner).

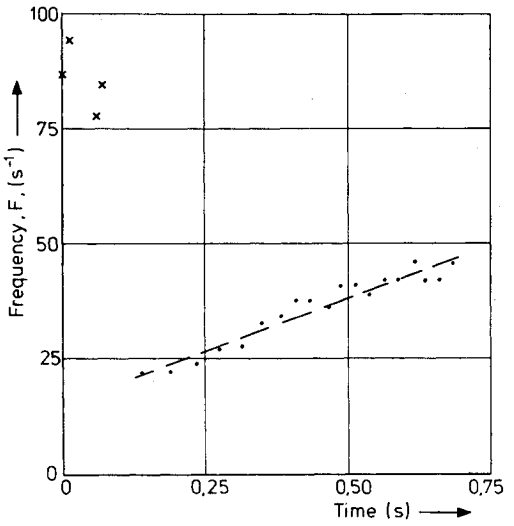

Fig. 9 Oscillation frequency of ARP propellant (10 cm L^* burner).

dampening constant:

$$\alpha_{\text{eff}} = \alpha - \alpha_d \tag{8}$$

If the dampening constant is proportional to the chamber volume or the exposed wall surface area, then

$$\alpha_d = CT \tag{9}$$

C is a proportionality constant, and T stands for the chamber volume or the exposed wall surface area. The propellant growth constant may be estimated from two more or less similar tests 1 and 2:

$$\alpha = (\alpha_{\text{eff}_1} T_2 - \alpha_{\text{eff}_2} T_1)/(T_2 - T_1) \tag{10}$$

The best correlation is obtained if the dampening is assumed to be proportional to the gas volume, and the results are shown in Table 4. The values of the growth constants are

Table 4 Estimated ARP propellant growth constants

Frequency F, s^{-1}	Growth constant α, s^{-1}
~21	−2.84
~25	0.52
~30	1.38

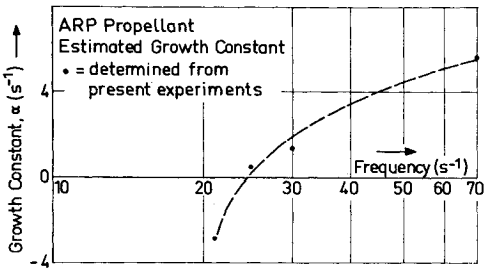

Fig. 10 Estimated growth constant of ARP propellant.

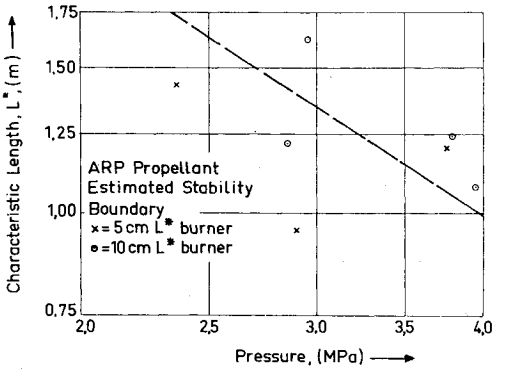

Fig. 11 Estimated stability boundary for ARP propellant.

of same order as the growth constant, $\alpha = 5.7$ s^{-1}, observed during test 955 at a mean frequency of 67 s^{-1} (see Table 3).

The growth constant α vs the frequency F is shown in Fig. 10: below ~ 25 Hz, $\alpha < 0$ which implies that any oscillation below this frequency is dampened, even if there are no other dampening mechanisms. According to Fig. 10, above ~ 25 Hz the propellant will drive the oscillations.

It was observed (cf. Figs. 6 and 7) that the oscillations decay with increasing L^* and it appears logical to assume that past the point where the oscillations seem to disappear or merge with the noise there will be no further appreciable oscillations. Kumar[9] defines "the point where the pressure amplitude merges with the noise level in the time-independent combustion" as a locus of the stability boundary in the $L^* - \bar{p}$ plane. Such a stability boundary for ARP propellant is shown in Fig. 11. Although the results are not very convincing, the scatter between data of the 5 and 10 cm burners is not larger than the scatter in the data of one type of burner. Moreover, the scatter does not appear to be worse than observed in similar stability plots.[9] This seems to imply that for ARP propellant dampening is of only minor importance insofar as the stability boundary is concerned.

Chuffing was observed in many cases, sometimes preceding oscillatory combustion, but many times only chuffing took place and often more than 100 times in succession. In those cases where oscillatory combustion was preceded by chuffing, it was noted that this was either by a few chuffs (4-6) or by a great many (81).

Regions where chuffing and oscillatory combustion were observed are mapped in the $L^* - \bar{p}$ plane, as depicted in Fig. 12, and it is evident that there is an overlap of the regions where chuffing and oscillatory combustion may be expected with ARP propellant.

Oscillatory combustion with ARP propellant may occur for 0.15 MPa $< \bar{p} <$ 4 MPa and 0.25 m $< L^* <$ 1.6 m.

A strong correlation was found to exist between the frequency and the mean pressure of the oscillations as illustrated in Fig. 13. There exist two relations between the mean pressure and the frequency at which the oscillations take place: a low-pressure high-frequency relation ($\bar{p} <$ 0.4 MPa), and a medium-pressure low-frequency relation (1.25 $< \bar{p} <$ 4

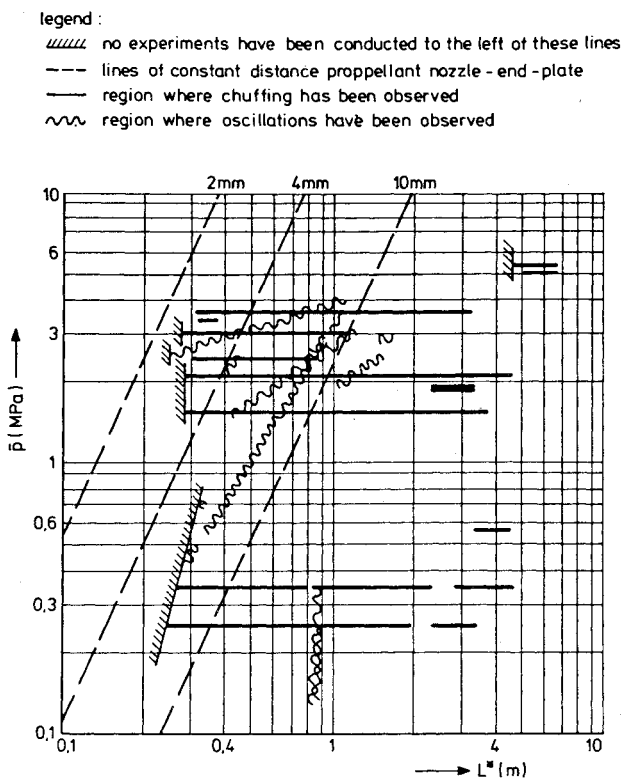

Fig. 12 L^* instability of ARP propellant: chuffing and oscillatory combustion.

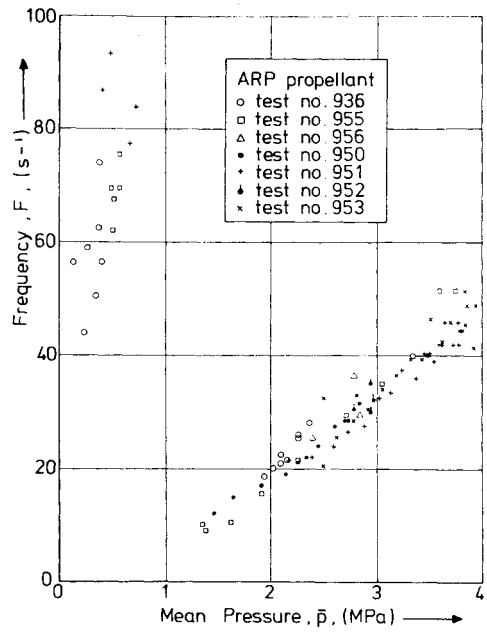

Fig. 13 Observed correlation between mean pressure and oscillation frequency of ARP propellant.

MPa). Only the medium-pressure low-frequency relation was reported ealier,[11,12] but not for the large pressure range found in the present experiments. Moreover, it is evident from Fig. 13 that the $\bar{p} - F$ correlation is the same for both the 5 and 10 cm L^* burners. The open plotting symbols (circle, square, and triangle) indicated experiments with the 5 cm L^* burner, and the other plotting symbols indicate the 10 cm L^* burner. The low-pressure high-frequency oscillations may be of a somewhat different character and may perhaps be related to flame spreading, but this was not investigated.

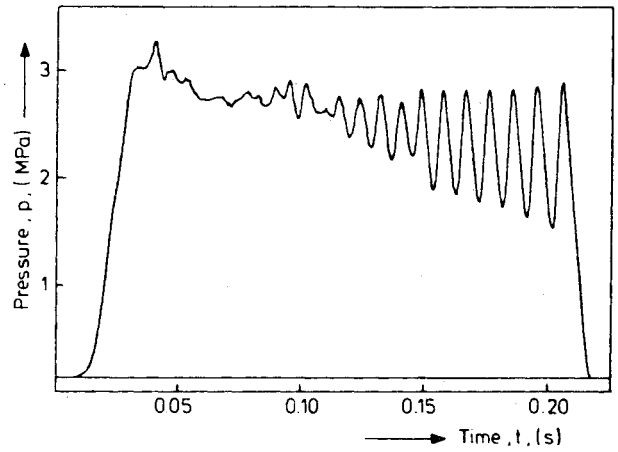

Fig. 14 L^* oscillations of ANP-2830 propellant (10 cm L^* burner).

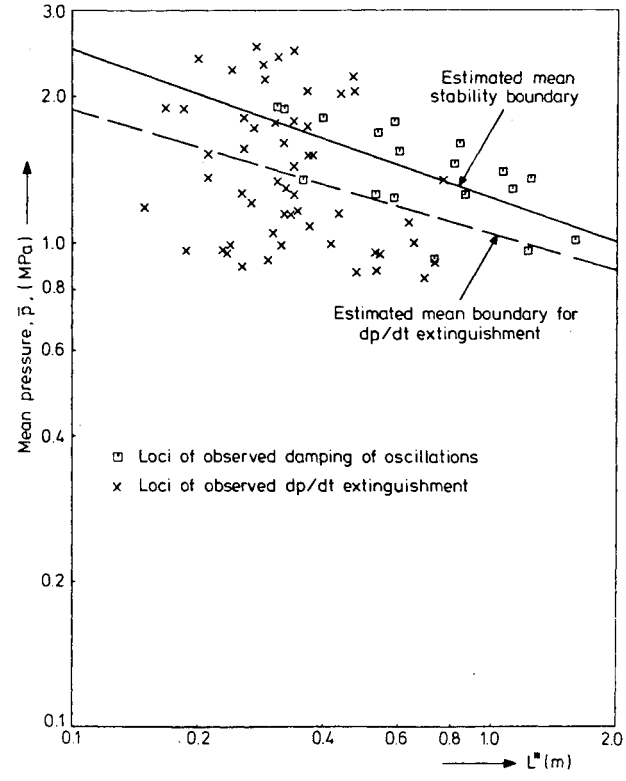

Fig. 15 Estimated stability boundaries for ANP-2830 propellant.

Composite Propellants

The experiments with composite propellants used a polyurethane propellant ANP-2830 with the composition listed in Table 5. More than 60 test runs were conducted of which more than 30 showed oscillatory combustion. Frequently dp/dt extinguishment was observed followed by reignition, so that more than 80 different pressure histories were obtained. Chuffing was not very prominent. Experiments used the 5 and 10 cm L^* burners and, as with double-base propellants, the results of both burners agree very well.

In the majority of cases the pressure histories which showed L^* oscillations displayed a more or less regular rise in pressure and after a short time oscillations with a growing amplitude appeared followed by dp/dt extinguishment. Often reignition took place and the sequence repeated itself. In some cases four successive repetitions were observed. In 18 cases, following increasing oscillation amplitudes, the amplitude leveled off and then decayed. Fig. 14 shows a typical pressure history. The difference with the pressure histories for ARP propellant

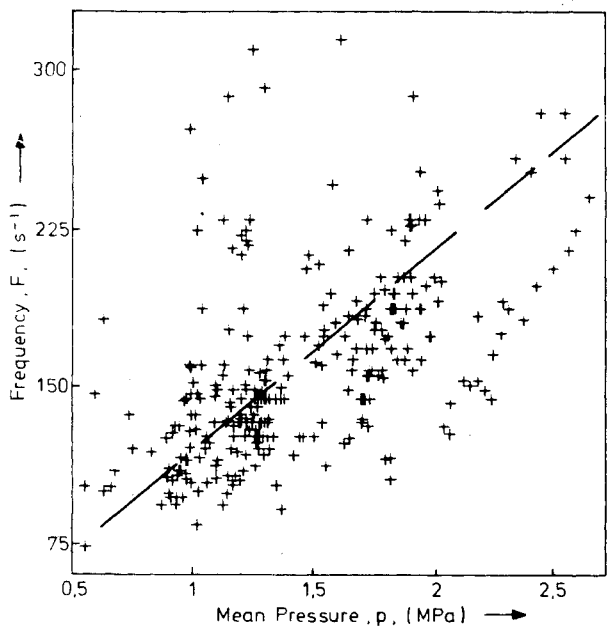

Fig. 16 Correlation between mean pressure and frequency during L^* oscillations of ANP-2830 propellant.

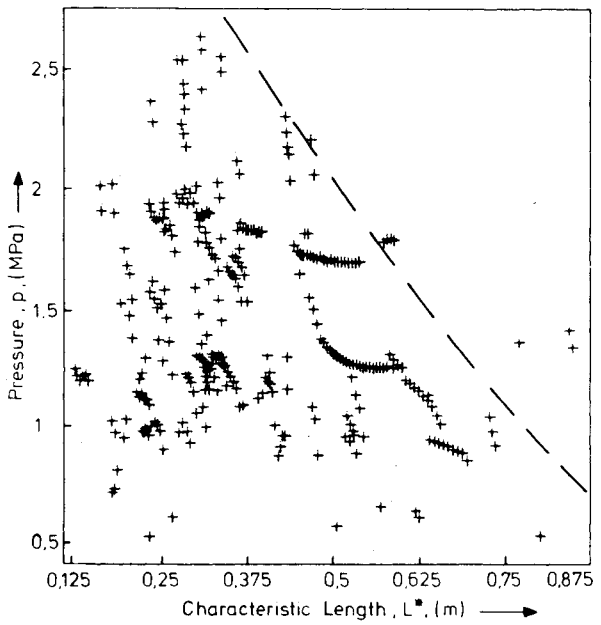

Fig. 18 Mean pressure during regular sustained L^* oscillations of ANP-2830 propellant.

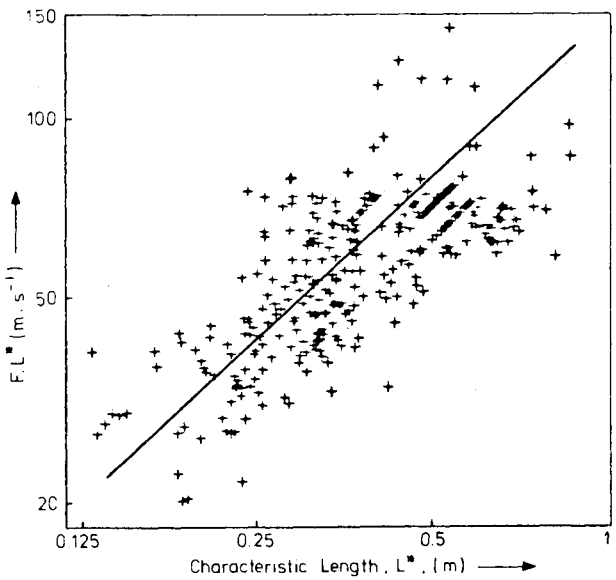

Fig. 17 Correlation between FL^* and L^* for ANP-2830 propellant.

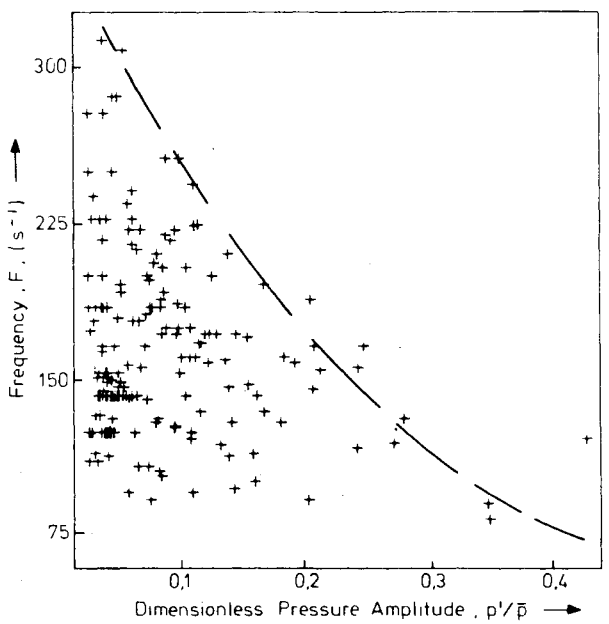

Fig. 19 Relation between frequency and normalized pressure amplitude during regular sustained L^* oscillations of ANP-2830 propellant.

Table 5 Composition (wt. %) of ANP-2830 propellant

AP	74
Polyurethane	19.39
Aluminium	6
Burning rate catalyst	0.55
Cure catalyst	0.06

is obvious, oscillations started with a small amplitude and there was no low-level pressure plateau with higher frequency oscillations.

Not all data are suitable for immediate detailed analysis. In some cases the oscillations were irregular or not sustained, therefore a selection was made between regular, sustained oscillations which are suitable for immediate preliminary analysis and other data which require a "second look."

From all available data a compilation was prepared of the loci of points where dp/dt extinguishment was observed, and the loci of points where the oscillation disappeared due to dampening. These loci are plotted in Fig. 15. From the loci of points where the amplitude of the oscillation disappears in the noise of the steady signal, a "mean stability boundary" (MSB) was estimated using a linear regression technique and is plotted in Fig. 15 as a solid line. In the same way a "mean boundary for dp/dt extinguishment" (MBE) was estimated from the loci of points where dp/dt extinguishment was observed and is plotted as a dashed line. It should be noted that:

1) The MSB and the MBE are almost parallel.

2) The majority of the loci for dampening of oscillations lies above the MBE. As dp/dt extinguishment occurred in the case of rapidly growing amplitudes, this is understandable.

3) There was a tendency for dp/dt extinguishment to take place at lower L^* values, while damping of oscillations has the tendency to occur at somewhat larger L^* values.

For the sustained and regular oscillations, a preliminary analysis reveals interesting results. Fig. 16 shows the observed frequency vs mean pressure for these experiments. Although the scatter was larger than for the ARP propellant (Fig. 13) again a correlation between F and $\bar{p}$ is evident, confirming that the $F-\bar{p}$ correlation may hold for both double-base and composite propellants.[13] A "low-pressure high-frequency" branch, however, was not observed for this composite propellant and the frequencies here were much higher than in the case of ARP propellant.

The imaginary part of the response function of a propellant is related to the product FL^* [6]:

$$R_b^{(i)} = 2\pi FL^*/(\gamma\Gamma\sqrt{RT_c}) \tag{11}$$

From Fig. 17 it is evident that a correlation exists between FL^* and L^*. No correlation could be traced between FL^* and $\bar{p}$, which may indicate that the imaginary part of the response function is only a weak function of the mean pressure.

In Fig. 18 the mean pressure during oscillations is plotted vs L^* for regular sustained oscillations. It is seen that the majority of the regular sustained oscillations takes place in an area roughly bounded by

$$\bar{p} = 4 - 3.8\,L^* \tag{12}$$

where $\bar{p}$ is in MPa and L^* is in m.

For regular, sustained oscillations Fig. 19 shows the ratio of the pressure amplitude and mean pressure $\Delta p/\bar{p}$ vs the frequency F. It is seen that at low frequencies, pressure fluctuations of more than 30% of the mean pressure may occur, but at higher frequencies only small pressure oscillations were observed.

Conclusions

1) L^* instability may be triggered by ignition peaks. The size of the ignition peak may determine, among other courses, the type of the resulting L^* instability (chuffing, oscillatory combustion).

2) Reliable and reproducible propellant ignition can be achieved by use of a pyrotechnic lacquer paste and an electrical resistance wire.

3) The size of the L^* burner has no noticeable influence upon the occurrence and type of L^* instability. Test runs in the 5 cm L^* burner were reproducible in the 10 cm L^* burner. This gives confidence to apply information obtained from L^* burner experiments to actual rocket motors.

4) ARP double-base propellant is sensitive to L^* instability in a region, approximately bounded by $\bar{p} = 3.91(L^*)^{-0.91}$ ($\bar{p}$ in MPa, L^* in m).

5) ANP-2830 propellant is sensitive to L^* instability in a region, approximately bounded by $\bar{p} = 1.26\ (L^*)^{-0.31}$ ($\bar{p}$ in MPa, L^* in m).

6) There is a correlation between the mean pressure during L^* oscillations and the frequency.

7) For ANP-2830 composite propellant a correlation exists between the imaginary part of the response function and the characteristic length.

8) There is a pronounced difference between the observed amplitude histories during oscillatory combustion of ARP double-base propellant and ANP-2830 composite propellant. For ARP propellant the amplitude initially has a large value and decays continuously, for ANP-2830 propellant the amplitude grows from an initially small value.

Acknowledgments

This work has been carried out in cooperation with the Prins Maurits Laboratory of the National Defense Organization, TNO.

References

[1] Akiba, R. and Tanno, M., "Low Frequency Instability in Solid Propellant Rocket Motors," *Proceedings of First Symposium (International) on Rockets and Astronautics, Tokyo, 1959,* Yokendo Tokyo, 1960, pp. 74-82.

[2] Sehgal, R. and Strand, L., "A Theory of Low-Frequency Combustion Instability in Solid Rocket Motors," *AIAA Journal*, Vol. 2, April 1964, pp. 696-702.

[3] Oberg, C.L., "Combustion Instability: The Relationship between Acoustic and Non-acoustic Instability," *AIAA Journal*, Vol. 6, Feb. 1968, pp. 265-271.

[4] Culick, F.E.C., "Some Nonacoustic Instabilities in Rocket Chambers Are Acoustic," *AIAA Journal*, Vol. 6, July 1968, pp. 1421-1423.

[5] De Boer, R.S. and Schöyer, H.F.R., "Results of L^* Instability Experiments with Double Base Rocket Propellants," Delft University of Technology, Dept. of Aerospace Engineering/Technological Laboratory TNO, Delft/Rijswijk, The Netherlands, Report LR-224/Report No. TL R 3050-1, 1976.

[6] Schöyer, H.F.R., "Report on Low-Frequency Oscillatory Combustion Experiments," Daniel and Florence Guggenheim Jet Propulsion Center, California Institute of Technology, Pasadena, 1971.

[7] Kuentzmann, P. and Lengellé, G., "Recent Research Activity at ONERA on Combustion Instability and Erosive Burning," ONERA, Chatillon, France, Technical Paper 1977-30, 1977.

[8] Ambrosius, B.A.C., "Eerste Aanzet tot een Rekenprogramma voor het Automatisch Verwerken van Meetresultaten van L^* - Experimenten," Delft University of Technology, Dept. of Aerospace Engineering, Delft, The Netherlands, Memorandum M-275, 1977.

[9] Kumar, R.N., "Some Experimental Results on the L-Star Instability of Metallized Composite Propellants," AIAA Paper 75-226, 1975.

[10] De Boer, R.S., Schöyer, H.F.R., and Wolff, H., "Results of L^*-instability Experiments with Double Base Rocket Propellants II," Delft University of Technology, Dept. of Aerospace Engineering/Technological Laboratory TNO, Delft/Rijswijk, The Netherlands, Report LR-252/Report No. TL R 3050-II, 1977.

[11] Eisel, L.J., Horton, M.D., Price, E.W., and Rice, D.W., "Preferred Frequency Oscillatory Combustion of Solid Propellants," *AIAA Journal*, Vol. 2, July 1964, pp. 1319-1323.

[12] Yount, R.A. and Angelus, T.A., "Chuffing and Non-acoustic Instability in Solid Propellant Rockets," *AIAA Journal*, Vol. 2, July 1964, pp. 1307-1313.

[13] Schöyer, H.F.R., "L^* Oscillations and a Pressure-Frequency Correlation for Solid Rocket Propellants," *AIAA Journal*, Vol. 15, Sept. 1977, pp. 1347-1348.